

Specification of Sea Surface Temperature Anomaly Patterns in the Eastern North Pacific¹

NATHAN E. CLARK

Southwest Fisheries Center, National Marine Fisheries Service, NOAA, La Jolla, Calif. 92037

(Manuscript received 31 January 1972, in revised form 14 April 1972)

ABSTRACT

Observed changes in sea surface temperature anomaly patterns on monthly and seasonal time scales are related to anomalous circulation patterns in the overlying atmosphere using data collected from the eastern North Pacific over a 10-year period (1961–70). Three monthly (November 1969, December 1969, January 1970) and four seasonal (fall 1969, winter 1969–70, spring 1970, summer 1970) case studies are described which show that the observed anomalous temperature changes can be explained quite well by relating them to anomalous heat transfer across the air-sea interface and heat advection by anomalous wind-driven ocean surface currents. These interactions are documented by charts showing the anomaly patterns of sea surface temperature change, sea level pressure, types of heat transfer across the air-sea interface, and wind drift currents. In addition, correlations computed between the anomaly patterns for each of the periods studied show that the interactions hypothesized have statistical significance. Although only seven case studies are described, the results are representative of those for most of the other months and seasons in the 10-year period.

An analysis of several years of data from Station PAPA (50N,145W), which included observed mixed layer depth values, indicates that between-year fluctuations in mixed layer depths can have a large effect in determining anomalous sea surface temperature changes, particularly when new seasonal thermoclines are forming. These effects should be included in any method used to specify (or predict) anomaly changes in order to avoid the relatively large errors that can occur from using long-term mean values.

1. Introduction

In a series of papers, Namias (1959, 1963, 1965, 1969, 1970, 1971) has shown that air-sea interaction processes can play an important role in determining the thermal structure and circulation characteristics of both ocean and atmosphere on monthly and seasonal time scales. Anomalous thermal or circulation patterns in either medium can create, amplify or destroy anomalous patterns in the other. These interactions occur on a contemporary or lag basis in time and over large (ocean-wide) spatial scales. The importance of understanding these interaction processes is now recognized as essential before meaningful long-range forecasting of atmospheric and oceanic properties can be made.

Most of Namias' studies presented qualitative and statistical results in defining the nature of air-sea coupling, although several of his reports (1959, 1963, 1965) and those of Eber (1961), Clark (1967) and Jacob (1967) described techniques that attempted to explain quantitatively the changes that occur in sea surface temperature anomaly patterns on monthly and seasonal time scales. The purpose of this paper is to show, by describing several case studies in both a qualitative and quantitative manner, that these observed anomalous changes can be related to well-known, large-scale, air-sea interaction processes.

It is important to note that this is an empirical study of these interaction processes. The methods used to describe and compute their effects are ones that consistently gave the best results in anomaly specification, with "best results" meaning the most significant positive pattern correlations and smallest rms errors between the computed and observed anomaly fields.

It is also noted that the specification procedure in this study is essentially the same as the one used by Clark (1967) to describe the anomalous fluctuations of sea surface temperature in the North Pacific throughout the 1951–57 period. The results reported here can be thought of as a verification of the ideas introduced in that study since they were obtained from a set of data that is independent of the set initially used to develop the specification procedure.

2. Development of the specification method

For a column of water of unit cross-sectional area and of depth D (z positive upward), the heat balance equation may be written as

$$\int_0^t \int_{-D}^0 \left(\rho C_p \frac{\partial T}{\partial t} \right) dz dt = \int_0^t \int_{-D}^0 Q_v dz dt + \int_0^t (Q + Q_D) dt, \quad (1)$$

¹ Presented at the Conference on the Interaction of the Sea and the Atmosphere, 1–3, December 1971, Ft. Lauderdale, Fla.

where T is the temperature of the water, Q the total heat transfer across the air-sea interface, Q_v the horizontal advection of heat into the column, and Q_D the vertical flux of heat into the column at depth $-D$. Since horizontal temperature gradients are small in most ocean areas, heat flux due to lateral diffusion is assumed to be negligible compared to the other heat exchange processes and is not included in (1). This equation expresses the relationship over the time interval t between the storage of heat in the column and the total exchange of heat energy between the column and its environment.

The differential form of (1) can be written as

$$\partial T / \partial t = -\mathbf{v} \cdot \nabla T + q, \quad (2)$$

where $-\mathbf{v} \cdot \nabla T = Q_v / (\rho C_p)$ and $q = Q / (\rho C_p z)$. The effects of Q_D are neglected because of a lack of adequate data to determine its importance in anomaly specification. However, order-of-magnitude estimates made from anomaly values of vertical velocity at the bottom of the Ekman layer and representative temperature lapse rates in the eastern North Pacific indicate that these effects are an order of magnitude less than the effects due to horizontal heat advection and heat transfer across the air-sea interface.

Following a method introduced by Arthur (1966) and modified by Clark (1968), let (2) be re-written as

$$D\theta / Dt = q, \quad (3)$$

where θ is the temperature of the upper mixed layer of the ocean and is assumed to be independent of depth, q is the rate of change of temperature of the layer due to non-advective processes, and D/Dt is the operator

$$\frac{D}{Dt} = \frac{\partial}{\partial t} + u \frac{\partial}{\partial x} + v \frac{\partial}{\partial y} + w \frac{\partial}{\partial z}.$$

Throughout the rest of the paper, the term "sea surface temperature" will refer to the temperature θ of the upper mixed layer or quasi-isothermal layer above the seasonal thermocline.

Letting θ, u, v, w, q be expressed in the forms $\theta = \bar{\theta} + \theta'$, $u = \bar{u} + u'$, $v = \bar{v} + v'$, $w = \bar{w} + w'$, $q = \bar{q} + q'$, where the capital letters denote long-term averages of the quantities for a particular location and month and the primed terms individual monthly deviations from these averages, the equivalent form of (3) is

$$\begin{aligned} \frac{\partial(\bar{\theta} + \theta')}{\partial t} = & -(\bar{u} + u') \frac{\partial(\bar{\theta} + \theta')}{\partial x} - (\bar{v} + v') \frac{\partial(\bar{\theta} + \theta')}{\partial y} \\ & - (\bar{w} + w') \frac{\partial(\bar{\theta} + \theta')}{\partial z} + (\bar{q} + q'). \quad (4) \end{aligned}$$

If a horizontal bar over a product of terms indicates that an average value of the product has been computed over all available data for a particular month, the

normal or long-term mean value of (4) becomes

$$\begin{aligned} \frac{\partial \bar{\theta}}{\partial t} = & - \left[\bar{u} \frac{\partial \bar{\theta}}{\partial x} + \bar{v} \frac{\partial \bar{\theta}}{\partial y} + \bar{w} \frac{\partial \bar{\theta}}{\partial z} \right] \\ & - \left[\overline{u' \frac{\partial \theta'}{\partial x}} + \overline{v' \frac{\partial \theta'}{\partial y}} + \overline{w' \frac{\partial \theta'}{\partial z}} \right] + \bar{q}. \quad (5) \end{aligned}$$

Subtracting (5) from (4) and integrating the result from time t_1 to t_2 (neglecting the effects of vertical motion), the following equation relates the change in sea surface temperature anomaly between times t_1 and t_2 to the effects of horizontal advection of sea surface temperature and non-advective heat transfer during this period:

$$\begin{aligned} \theta'(t_2) - \theta'(t_1) & \\ (a) & \\ = & - \int_{t_1}^{t_2} [\bar{u} \partial \theta' / \partial x + \bar{v} \partial \theta' / \partial y] dt \\ (b) & \\ & - \int_{t_1}^{t_2} [u' \partial \theta' / \partial x + v' \partial \theta' / \partial y] dt \\ (c) & \\ & - \int_{t_1}^{t_2} [u' \bar{\theta} / \partial x + v' \bar{\theta} / \partial y] dt \\ (d) & \\ & + \int_{t_1}^{t_2} [\overline{u' \partial \theta' / \partial x} + \overline{v' \partial \theta' / \partial y}] dt + \int_{t_1}^{t_2} q' dt. \quad (6) \quad (e) \end{aligned}$$

Integral (a) in (6) represents the change in sea surface temperature anomaly (or anomalous change in sea surface temperature) over the period t_1 to t_2 due to the interaction between the mean surface current and the anomalous temperature gradients; integral (b) represents the interaction between the current and gradient anomalies; integral (c) represents the interaction between the current anomalies and the mean temperature gradient; integral (d) represents an effect involving possible correlations between the current and gradient anomalies; and integral (e) represents the effect of anomalous heat transfer across the air-sea interface.

Integral (c) in (6) can also be identified with the procedure introduced by Namias (1965) and used by Jacob (1967) to specify the change in sea surface temperature anomalies over an interval $t_2 - t_1$ of one month. Clark (1968) evaluated the relative magnitudes of the first four integrals in (6) using seven years (1951-57) of monthly averaged data over the North Pacific from 20 to 60N. His results showed that the contribution of integral (c) to (6) predominates between 30-45N, and it is in this region that Namias and Jacob obtained their best results. In higher or lower latitudes, integrals (a) and (b) become important, while integral (d) involving

the correlation terms is small relative to the others and may be neglected.

The computational methods used in the present study to specify changes in θ' implicitly involve all five integrals in (6), thus including the effect of heat transfer across the air-sea interface [the integral (e)].

3. Heat transfer processes and data used in their computation

a. Formulation of the heat transfer equations

The total heat transfer across the air-sea interface Q (positive when the ocean surface layer is gaining heat) may be written as the downward flux of solar radiation Q_i minus the sum of the upward flux of longwave or back radiation Q_b , evaporative or latent heat transfer Q_e , and conductive or sensible heat transfer Q_s , or

$$Q = Q_i - (Q_b + Q_e + Q_s). \quad (7)$$

The terms on the right side of (7) are functions of time, cloud cover over the ocean surface, wind speed over the surface, and the air-sea difference of temperature and vapor pressure. The formulas used in determining the values of these terms are those given in Johnson *et al.* (1965).

The horizontal advection of heat Q_e at depth $-z$ may be written as

$$Q_e = -\rho C_p (\mathbf{v}_e \cdot \nabla T), \quad (8)$$

where ρ is the density of sea water, C_p the specific heat of sea water at constant pressure, \mathbf{v}_e the horizontal current velocity at depth $-z$, and ∇T the horizontal gradient of temperature at the same depth.

The results in the empirical studies of Namias (1959, 1965), Clark (1967) and Jacob (1967) indicate that the best method of specifying anomalous changes in sea surface temperature from horizontal advective processes is to use an expression first proposed by Ekman for the magnitude of the surface current velocity \mathbf{v}_c , i.e.,

$$v/w = 0.0127 / (\sin \phi)^{1/2}, \quad (9)$$

where v is the magnitude of the surface current, w the magnitude of the geostrophic wind, and ϕ the latitude value at a computational gridpoint. It is assumed in this method that winds near the ocean surface are capable of driving a surface layer of nearly isothermal water at some angle to the direction of wind flow.

Values of the average speed of the upper wind-mixed layer of the ocean were also computed from surface wind stress data using the equations that describe Ekman transport. The results were then used in conjunction with horizontal temperature gradients to obtain estimates of anomalous temperature changes due to horizontal heat advection. However, no consistent, significant correlations were found between the computed and observed anomalous change fields.

For the isothermal layer, (8) becomes

$$Q_e = -\rho C_p (u_c \theta_\lambda + v_c \theta_\phi), \quad (10)$$

where u_c and v_c are the east-west and north-south components of the surface current, and θ_λ and θ_ϕ are the east-west and north-south components of the horizontal temperature gradient of the isothermal layer.

From (9) the surface current components can be written as

$$u_c = 0.0127 (\sin \phi)^{1/2} (u_g \cos \alpha + v_g \sin \alpha), \quad (11a)$$

$$v_c = 0.0127 (\sin \phi)^{1/2} (v_g \cos \alpha - u_g \sin \alpha), \quad (11b)$$

where u_g and v_g are the east-west and north-south components of the geostrophic wind, and α is the angle between the geostrophic wind and the ocean surface current directions.

In computing u_g and v_g monthly averaged sea-level pressures and finite-difference approximations to the geostrophic wind equations in spherical coordinates were used. The horizontal gradients of surface layer temperature were computed from finite-difference approximations to the gradient relationships in spherical coordinates, i.e., from

$$\theta_\lambda = (1/R \cos \phi) (\partial \theta / \partial \lambda) \approx (1/R \cos \phi) (\Delta \theta / \Delta \lambda), \quad (12a)$$

$$\theta_\phi = (1/R) (\partial \theta / \partial \phi) \approx (1/R) (\Delta \theta / \Delta \phi), \quad (12b)$$

where R is the earth's radius, and λ and ϕ denote longitude and latitude in radians. The grid spacing was 5° , so that $\Delta \lambda$ and $\Delta \phi$ were 10° or $(\pi/18)$ rad.

There has been a great deal of speculation as to what value should be used for the angle α between the geostrophic wind and the ocean surface current. Namias (1959, 1965), Jacob (1967) and Clark (1967) used 45° in their computations. However, in this study when anomalous temperature changes were computed from (11) and (12) using several values for α between -45° and $+45^\circ$ and the results compared with observed values, significantly better correlations between the two were obtained when the surface current was assumed to flow in the same direction as the geostrophic wind, i.e., α was equal to 0° . This result may be explained if the assumption is made that the wind at the ocean surface is nearly the same angle to the *left* of the geostrophic wind as the ocean surface current is to the *right* of the surface wind. The surface wind drift current would then flow in a direction that is almost parallel to that of the geostrophic wind.

b. Monthly averaged data

The marine weather observations used in this study have been collected and processed at the National Marine Fisheries Service's La Jolla Laboratory since early 1960. Monthly averages of these observations taken over the eastern North Pacific were computed by 5° latitude-longitude sections and used to determine

monthly averaged values of Q_i , Q_b , Q_e , Q_s and Q_v . A 10-year mean of each variable was computed for each 5° section and month, yielding 93 grid-point values for each variable and each month. The grid extended from $20\text{--}55^\circ\text{N}$ and westward from the coast to 180°W . Departures of the monthly averages from the 10-year means (anomalies) were then computed.

A monthly averaged value for any quantity V is written as

$$V = \bar{V} + V', \quad (13)$$

where V is the monthly averaged value, \bar{V} the 10-year mean value, and V' the monthly departure from the mean value or anomaly. This notation will be used throughout the paper to denote long-term means and anomalies unless otherwise explained.

The accuracy of the exchange formulas in determining the transfer of heat depends upon the validity of the assumptions underlying the theory, the accuracy of the observational data, and the manner in which the formulas are used to calculate the heat transfer. Since the formulas are nonlinear, the use of monthly mean data instead of daily or hourly values could lead to errors.

Since monthly averaged variables were the only ones

available over a large area and a sufficiently long time period, they were used in this study to compute the heat transfer values. However, Clark's (1967) calculations with daily averaged data from two weather ships in the North Pacific and Kraus and Morrison's (1966) work using data from weather ships stationed in the North Atlantic indicate that the errors involved in using this procedure are acceptable in studying large-scale, air-sea interaction processes.

Eq. (10), which is used to determine heat transfer by horizontal advection, is also nonlinear in nature, and the use of monthly mean data could again cause errors. Nonetheless, monthly averaged values were used in this study, and the results obtained and described in the following sections indicate that this data base is sufficient to show some of the ways in which advective processes affect anomalous changes in large-scale, sea surface temperature patterns.

c. Seasonally averaged data

In addition to the monthly averaged values, seasonal averages of the marine weather observations were computed by 5° latitude-longitude sections. These results were used to determine seasonal averages, 10-year mean

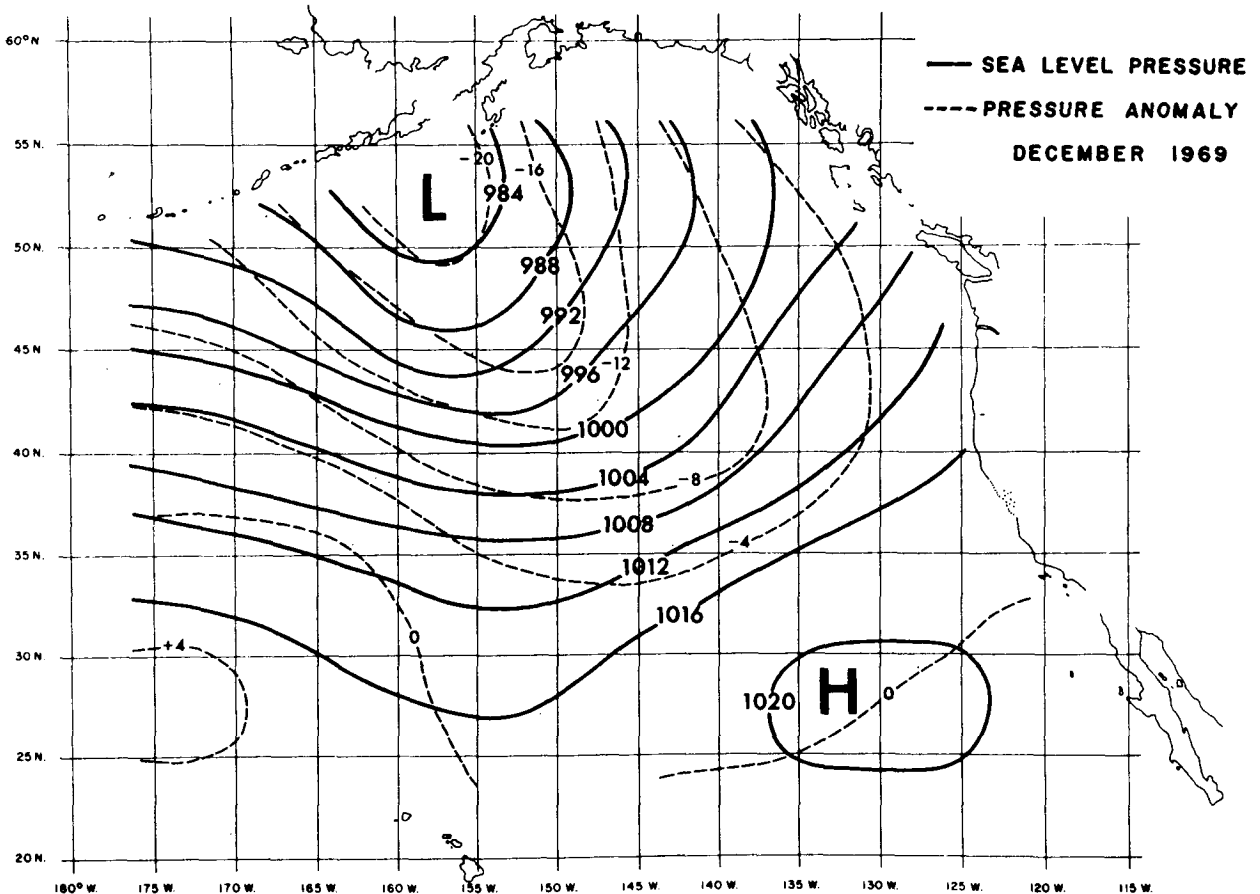


FIG. 1. Sea level isobars and anomaly isopleths (both in mb) for December 1969.

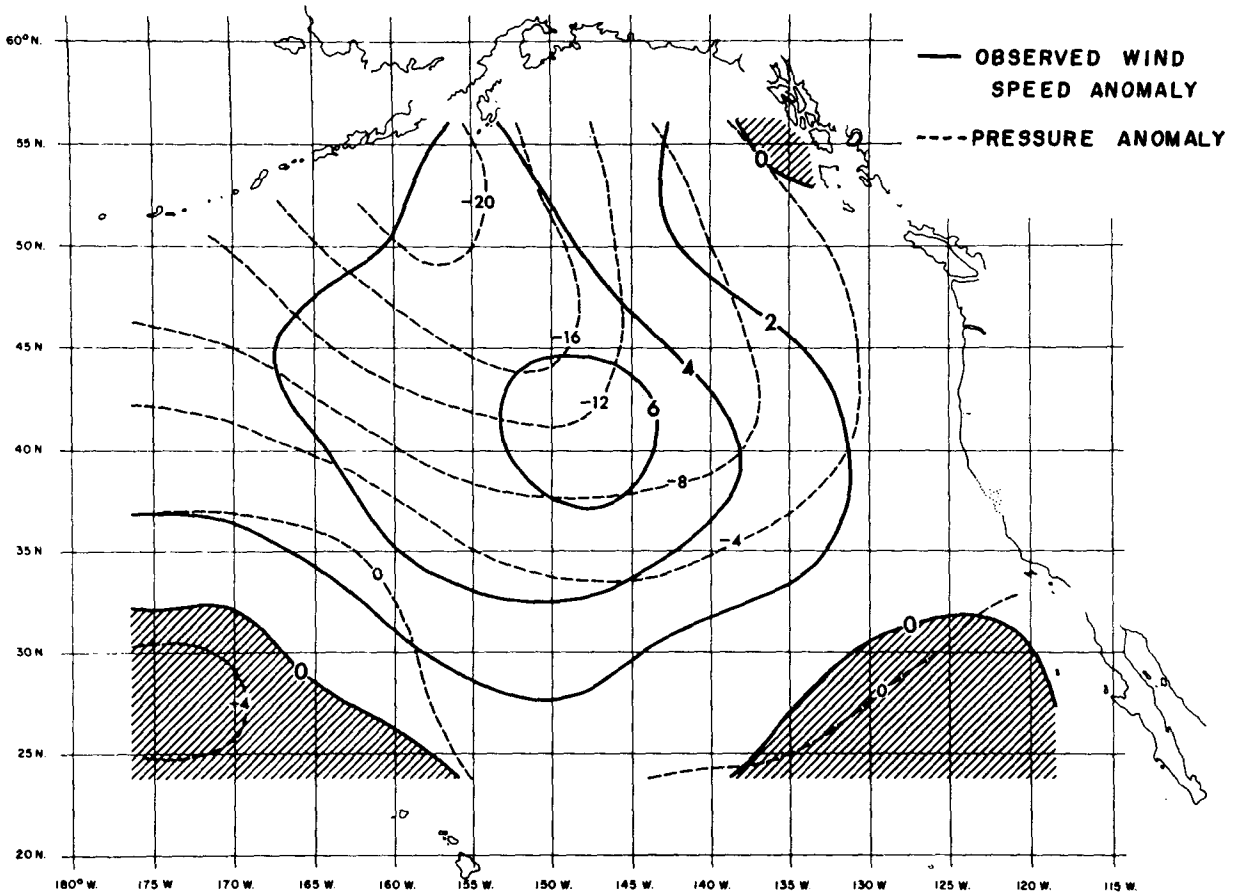


FIG. 2. Isopleths of observed wind speed anomaly (kt) and isopleths of sea level pressure anomaly (mb) for December 1969. Slant-shaded areas show regions of negative wind anomaly.

values, and seasonal anomalies for the same heat transfer terms that were computed using the monthly averaged variables. The 12 months were divided into four seasons, winter (December, January and February), spring (March, April and May), summer (June, July and August), and fall (September, October and November).

The discussion of inaccuracies caused by averaging procedures for the monthly averaged data also applies to the seasonally averaged values. In fact, the effects may be even more pronounced since longer time sequences are involved, at times, effectively masking important shorter term events. However, the high serial correlation found in sea surface temperature data (Namias, 1970) would seem to imply that seasonal means are quite indicative of the summation of daily effects.

4. Representative anomaly patterns of heat transfer processes

Fig. 1 shows the isobars of average sea level pressure (SLP) and the pressure anomaly pattern over the eastern North Pacific (ENP) for December 1969. The

negative departure of 20 mb south of the Alaskan Peninsula represents about three standard deviations from the 10-year mean and indicates the very strong cyclonic activity that occurred over the entire North Pacific during the month. A striking feature of the weather pattern over the ENP is its consistency throughout the month, with a negative 700-mb height anomaly of about 250 m (over three standard deviations from the mean) centered between 40–50N and 140–160W. The anomaly retained its intensity and configuration until the last week in December when it weakened and spread westward; however, the central region still had departures of almost two standard deviations from the mean (Posey, 1970).

The SLP anomaly pattern in Fig. 1 also shows the ways in which the anomalous atmospheric circulation during a month determines the general nature of the Q and temperature advection (TADV) anomaly patterns (Figs. 4 and 5). The orientation of the anomalous isobars indicates that cold, dry air moved into the eastern North Pacific from the northwest, causing increased evaporation and anomalous cooling of the ocean surface layer. These northwest winds also caused

anomalous cooling of the surface layer west of 150W through temperature advection. On the other hand, where the orientation of the isobars shows anomalous flow of warm, moist air from the south or southwest, the negative anomalies of evaporation are reduced in magnitude; the temperature advection anomalies are positive due to warmer water from the south having been transported northward by anomalous wind drift currents.

Fig. 2 shows the isotachs of anomalous observed (not geostrophic) surface wind speed along with the anomalous isobars. This superimposition of anomaly patterns points out several interesting relationships: 1) the observed wind speed anomalies (OBSW') are quite spatially coherent over the entire ENP; 2) the anomalies are positive over almost the entire region, indicating that the strong cyclonic activity during the month caused stronger than normal winds; and 3) the highest anomalous winds occurred in the same areas as the tightest anomalous pressure gradients, with maximum values (>6 kt) associated with the region of maximum atmospheric instability due to large air mass contrasts.

Since evaporative heat transfer Q_e is dependent upon wind speed, the large values of OBSW' between lati-

tudes 30 and 40N and longitudes 135 and 150W explain the large negative values of Q_e' in this area (Fig. 3), even though the anomalous winds are from the south or southwest.

The anomaly pattern of total heat transfer across the air-sea interface is shown in Fig. 4. There is a strong resemblance between this pattern and that in Fig. 3, indicating the strong influence of anomalous Q_e on Q (pattern correlation between the values of Q' and Q_e' is 0.95, or the two patterns have 91% of their variances in common). This relationship is typical of those found in most late fall and winter months.

The positive Q' values in the eastern Gulf of Alaska are due to a combination of less than normal evaporative cooling and longwave back radiation Q_b' . The latter effect is related to above-normal cloud cover in this region associated with the frequent passage of storm systems. North of Hawaii, between 33 and 37N, the negative anomaly of $150 \text{ cal cm}^{-2} \text{ day}^{-1}$ represents an approximate change of -0.50C in the temperature of the ocean surface layer during the month.

The heat transfer due to horizontal advective processes is given by (10). If this equation is divided by ρC_p , the result expresses the change in sea surface

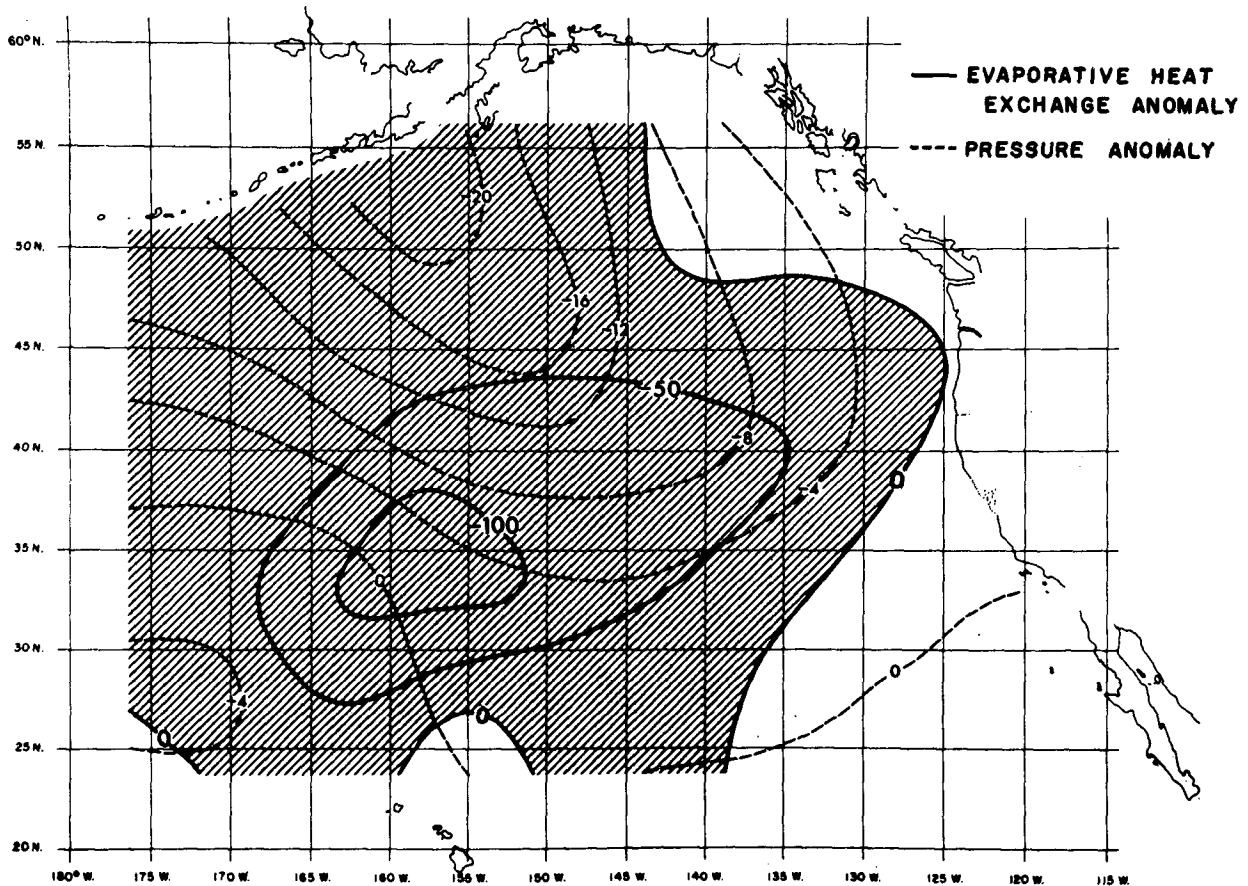


FIG. 3. Isopleths of evaporative heat exchange Q_e anomaly ($\text{cal cm}^{-2} \text{ day}^{-1}$) and isopleths of sea level pressure anomaly (mb) for December 1969. Slant-shaded area shows region of negative Q_e anomaly.

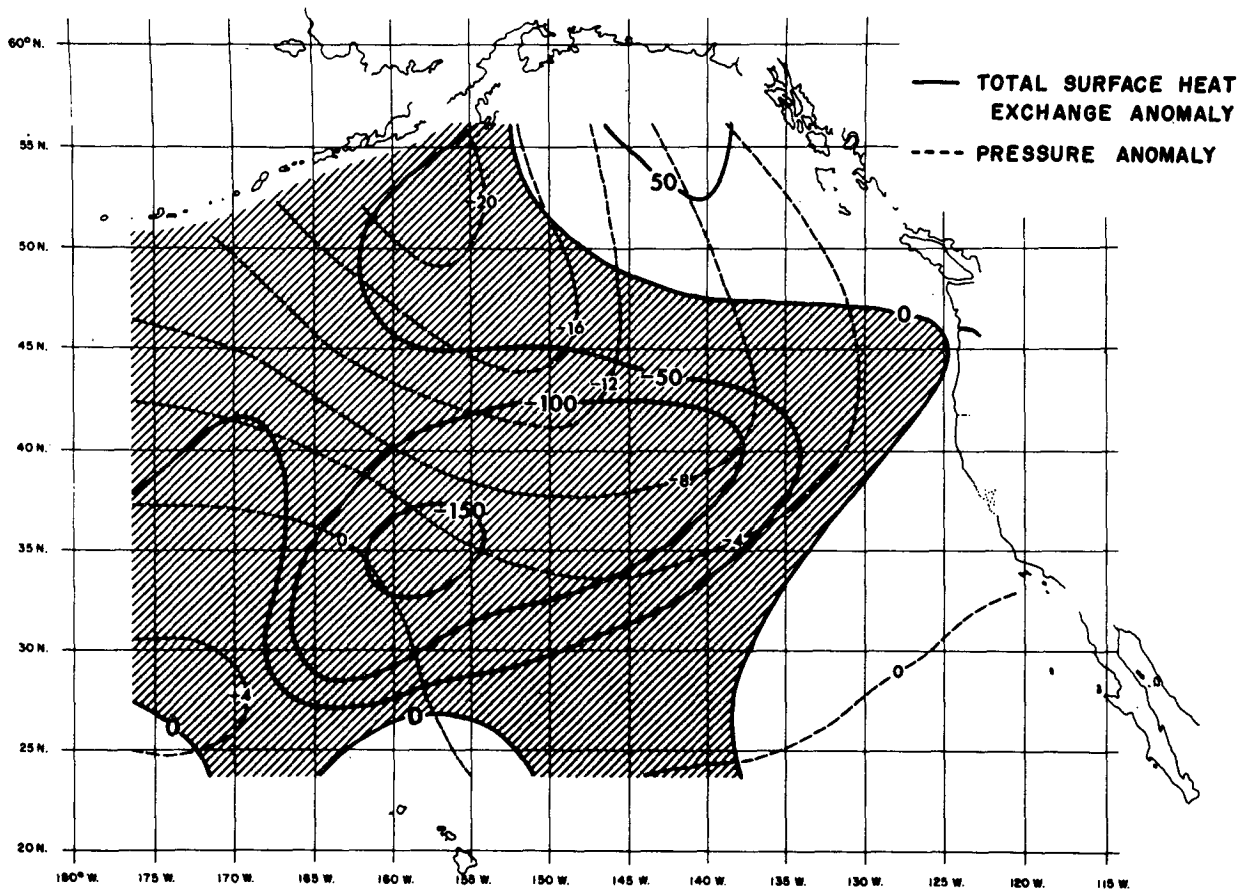


FIG. 4. Isopleths of total surface heat exchange Q anomaly ($\text{cal cm}^{-2} \text{ day}^{-1}$) and isopleths of sea level pressure anomaly (mb) for December 1969. Slant-shaded area shows region of negative Q anomaly.

temperature due to horizontal wind drift currents (TADV; anomalous value given by TADV'). The pattern of TADV' with the anomalous isobars superimposed for December 1969 is shown in Fig. 5. The results are as expected: negative anomalies in areas where the isobar orientation is from northwest to southeast, and positive anomalies in areas where the orientation ranges between southwest to northeast and southeast to northwest. Large positive and negative values of TADV' occur in regions of large OBSW', and the maximum value (about 0.75C per month) occurs where OBSW' is high, the surface isotherms run nearly west to east, and the anomalous isobars show anomalous winds from the south.

5. Relationships between anomalous changes in sea surface temperature patterns and heat transfer processes

a. Results using a monthly time scale

Three months, November and December, 1969, and January 1970, were chosen from the 10-year record of data to illustrate the types of large-scale air-sea interaction processes that occur and their effects on the

thermal characteristics of the upper mixed layer of the ocean. Although the results are shown for only three months, and those for only one month, December 1969, are described in detail, they are representative of most of the other months in the 10-year period.

In Section 2, changes in sea surface temperature anomalies were related to anomalies of temperature advection and non-advective heat transfer. If the long-term mean of (3),

$$\overline{(\partial\theta/\partial t)} = \overline{(-\mathbf{v}_e \cdot \nabla\theta)} + \bar{q}, \tag{14}$$

is subtracted from (3), those results can be represented by

$$(\partial\theta/\partial t)' = (-\mathbf{v}_e \cdot \nabla\theta)' + q'. \tag{15}$$

The term on the left side of (15) represents the anomalous time-rate-of-change of sea surface temperature θ at some location in the ocean and is affected by anomalous horizontal advective processes $(-\mathbf{v}_e \cdot \nabla\theta)'$ or TADV' and non-advective heat flux across the air-sea interface.

Since $q = Q/\rho C_p D$, values for q' in (15) can be determined from the values of Q' computed from (7). In converting the Q' values into anomalous temperature changes q' of the ocean surface layer, the assumption

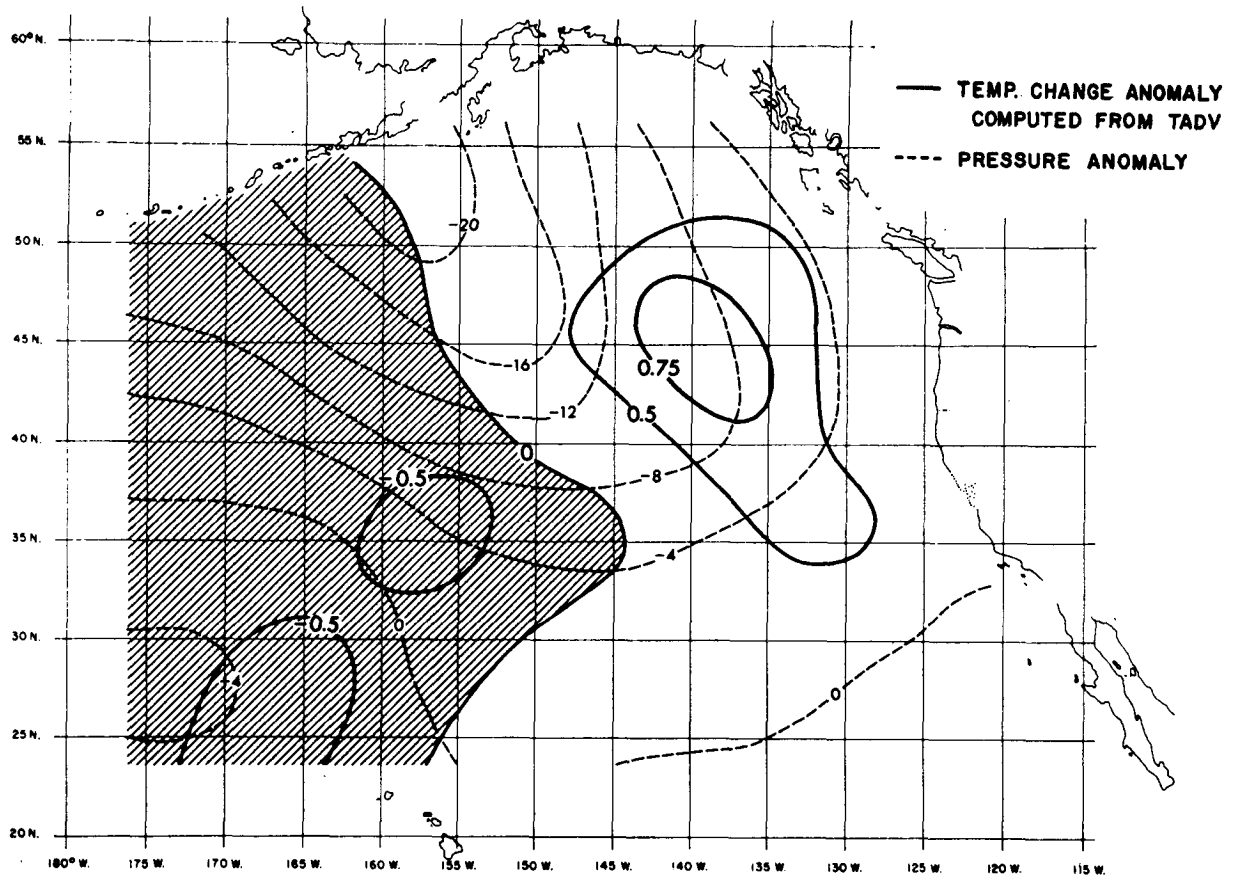


FIG. 5. Isopleths of sea surface temperature change anomaly ($^{\circ}\text{C}$) computed from horizontal temperature advection TADV and isopleths of sea level pressure anomaly (mb) for December 1969. Slant-shaded area shows region of negative TADV anomaly.

was made that the heat gained or lost is distributed evenly throughout a layer of depth D . The Q' values were then divided by $\rho C_p D$ to get the corresponding temperature change anomalies. Long-term mean values of the mixed layer depth D given by Pattullo and Cochrane (1951) were used in making these computations since observed values were not available. Errors resulting from the use of this procedure are discussed in Section 6.

Next, the q' values were added to those of TADV' and the results compared to the anomaly patterns of two finite-difference approximations to $\partial\theta/\partial t$. These approximations are described in the Appendix and are denoted by $\Delta\theta_{i,i-1}$ and $\Delta\theta_{i+1,i-1}$. Figs. 6 and 7 show the anomaly patterns of $\Delta\theta'_{i,i-1}$ and $\Delta\theta'_{i+1,i-1}$ for December 1969, respectively. Although the two anomaly patterns differ in specifics, there is good correspondence in their pattern configurations.

Fig. 8 shows the anomaly pattern of $\text{TADV}' + q'$ for December 1969. Visual comparison of the pattern in Fig. 8 with those in Figs. 6 and 7 shows that the anomalous temperature changes computed from anomalous advective and non-advective heat fluxes are often

twice the size of the estimated observed changes; however, their pattern configurations are quite similar.

In order to test the degree of similarity, linear correlations and rms differences were calculated between the values making up the patterns in Figs. 6–8. The results are shown in Table 1, with those for November 1969 and January 1970 included for comparison. These two months were different from December in that their anomalous atmospheric circulation patterns were not as consistent (Green, 1970; Wagner, 1970). Therefore, atmospheric events occurring on shorter time scales than 30 days probably had effects on the thermal characteristics of the ocean surface layer, and monthly averaged properties of the two media would not be expected to show a high degree of correlation.

The results show the highest pattern correlations and the smallest rms differences in December 1969. Depending on the scheme used to estimate $\partial\theta/\partial t$, the correlation coefficients are 0.81 (66% of variances in common) between $\Delta\theta'_{i,i-1}$ and $\text{TADV}' + q'$, and 0.66 (43% of variances in common) between $\Delta\theta'_{i+1,i-1}$ and $\text{TADV}' + q'$.

Both correlation coefficients greatly exceed the 1%

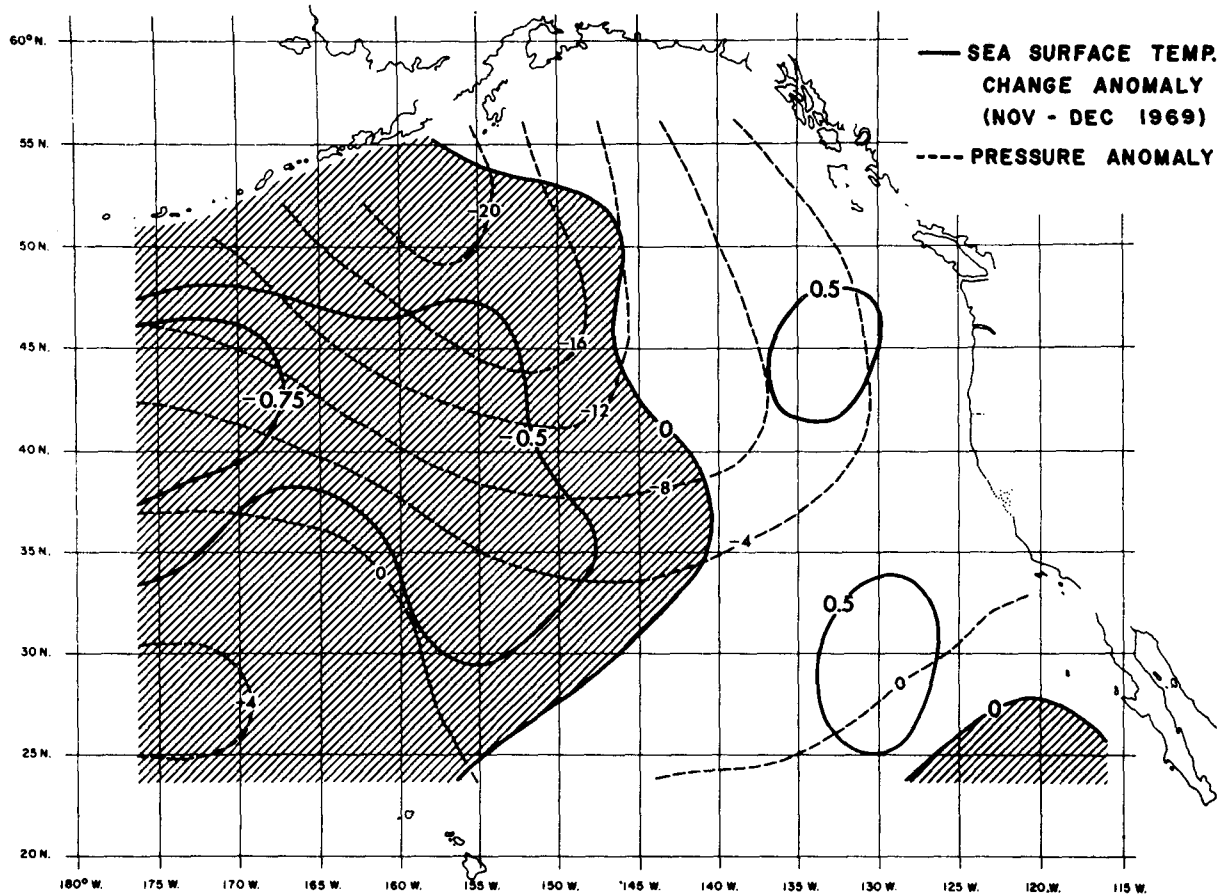


FIG. 6. Isopleths of observed sea surface temperature change anomaly ($^{\circ}\text{C}$) approximated using the backward finite-difference method and isopleths of sea level pressure anomaly (mb) for December 1969. Slant-shaded areas show regions of negative temperature change anomaly.

level of statistical significance (0.30) for 93 data points or 92 degrees of freedom. Since the values used in the correlations are not truly independent of each other, the 1% level should be higher than 0.30. However, positive correlations were consistently obtained using data for other months, and it is felt that the relationships indicated are real and not obtained by chance.

The correlations for November 1969 are lower than those for December 1969 but higher than those for January 1970. While all but two of the correlation coefficients equal or exceed the 1% (0.30) or the 5% (0.23) levels of statistical significance using the November 1969 results, none of them computed for January 1970 reach the 5% level. Descriptions of the atmospheric circulation patterns for the two months (Green, 1970; Wagner, 1970) show that the anomalous activity in November 1969 was more intense and consistent than that in January 1970.

For all three months, TADV' correlated better with $\Delta\theta'_{i, i-1}$, and q' correlated better with $\Delta\theta'_{i+1, i-1}$. Using this as a guide, it is seen from Table 1 that advective processes probably had a greater influence than non-

advective processes in determining the anomalous temperature changes in December 1969, while the reverse appears to be true in November 1969 and January 1970.

b. Results using a seasonal time scale

Table 2 shows the results of computing the same type of correlations discussed in the previous section except that seasonal rather than monthly data were used. The time periods chosen for study were fall 1969 (September, October and November, 1969), winter 1969-70 (December, 1969, January and February, 1970), spring 1970 (March, April and May, 1970), and summer 1970 (June, July and August, 1970). Again, as for the monthly data, the results are typical of the other seasons in the 10-year data record.

Of the four seasons, winter 1969-70 and spring 1970 show the highest correlations and the smallest rms differences. The correlations for summer 1970 are also high and represent the dominant influence of non-advective processes during this season. The correlations for fall 1969 are all quite low and reflect one or any combination of the following: 1) use of long-term mean

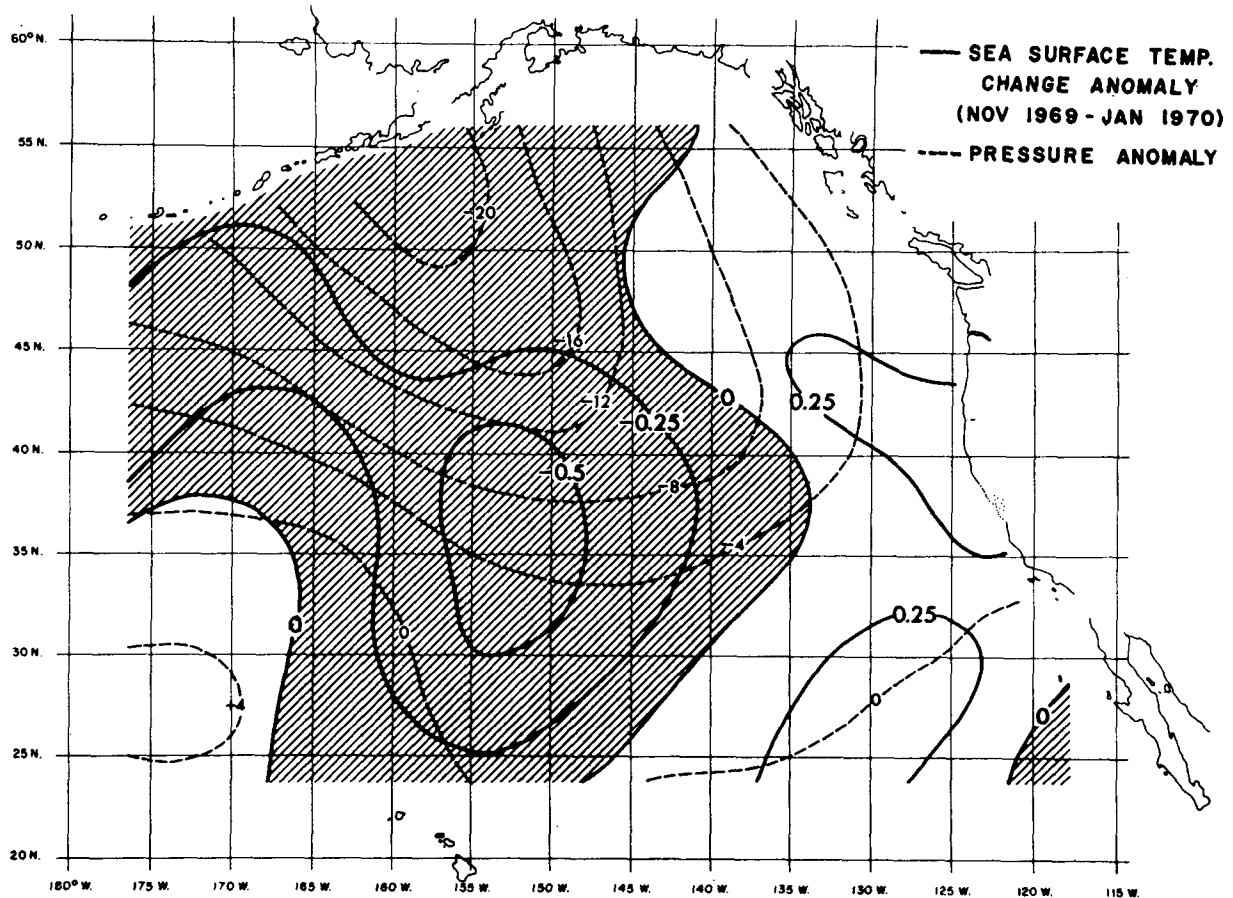


FIG. 7. Isopleths of observed sea surface temperature change anomaly ($^{\circ}\text{C}$) approximated using the centered finite-difference method and isopleths of sea level pressure anomaly (mb) for December 1969. Slant-shaded areas show regions of negative temperature change anomaly.

values for mixed layer depths; 2) seasons before and after biasing the estimations of $\partial\theta/\partial t$; and 3) exclusion of effects of other processes such as heat transfer across the seasonal thermocline. Correlations were computed using data for fall 1970 with essentially the same results.

From these results, it appears that advective heat transfer processes have a greater effect in determining anomalous sea surface temperature changes than non-advective processes in winter and spring, while the latter have a greater effect in summer and fall.

Comparisons were also made between the total heat transfer Q across the air-sea interface and the different processes contributing to the anomalous variations in Q . The pattern correlation coefficients in Table 3 indicate that: 1) during fall 1969, winter 1969-70 and spring 1970, anomalous changes in the evaporative heat transfer Q_e are mainly responsible for corresponding changes in Q ; 2) during summer 1970 the Q_e anomaly pattern is also highly correlated with the Q pattern, however, during this season anomalies in the incoming radiation Q_i play a major role in determining the Q anomaly pattern; and 3) the Q anomaly patterns are negatively correlated with those of cloud cover in

spring and summer 1970, reflecting the dependence of Q on Q_i during these seasons since increased cloud cover causes a decrease in radiation reaching the ocean surface. The correlation between the Q_e and observed wind speed anomaly patterns is smaller in summer 1970 than in the other three seasons, indicating that air-sea vapor pressure differences played a stronger role in determining evaporation during this period. These results are similar to those obtained for other years in the 1961-70 period.

6. Discrepancies between observed and computed anomalous sea surface temperature changes

In determining the anomalous changes in sea surface temperature patterns from the anomaly patterns of the total heat transfer across the air-sea interface or non-advective processes q , mean values of the mixed layer depth were used because observed monthly averaged values were not available over the entire eastern North Pacific. Since relatively large fluctuations of the monthly averaged values do occur between the same months of different years, the use of long-term mean values will

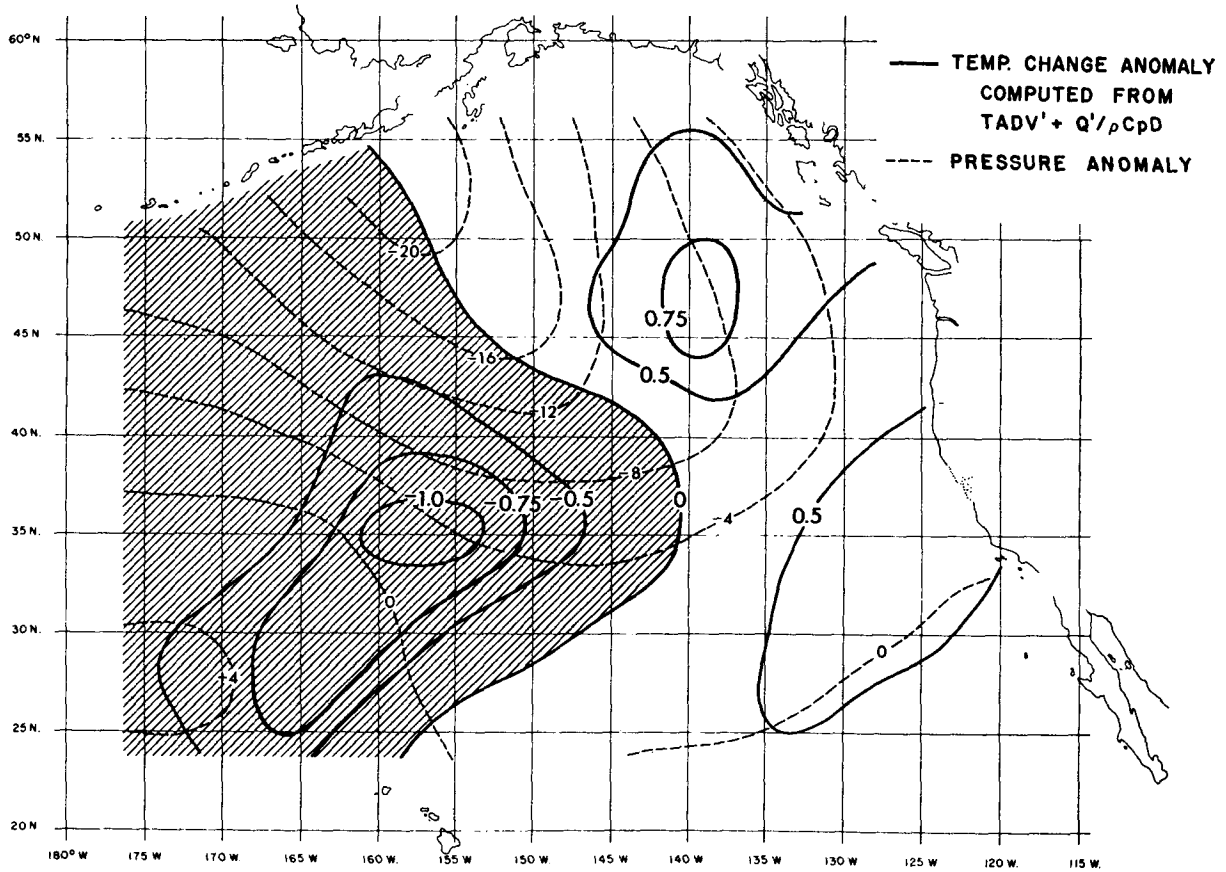


FIG. 8. Isopleths of sea surface temperature change anomaly ($^{\circ}\text{C}$) computed from temperature advection TADV and total surface heat transfer $Q/(\rho C_p D)$ and isopleths of sea level pressure anomaly (mb) for December 1969. Slant-shaded area shows region of negative TADV + $Q/(\rho C_p D)$ anomaly.

cause errors in specifying anomalous temperature changes in certain areas and at certain times of the year. The effects of using the long-term mean values instead of monthly averaged observed values can be demonstrated by the following:

Using (3) in the form

$$\partial\theta/\partial t = -\mathbf{v}_c \cdot \nabla\theta + Q/(\rho C_p D), \quad (16)$$

and letting $Q = \bar{Q} + Q'$ and $D = \bar{D} + D'$ where the bar denotes a long-term mean value and the prime a deviation from the mean value or anomaly, the second term on the right side of (16) can be written as

$$\begin{aligned} \frac{Q}{\rho C_p D} &= \frac{\bar{Q} + Q'}{\rho C_p (\bar{D} + D')} \\ &= \frac{(\bar{Q} + Q')}{\rho C_p \bar{D}} \left[1 - \frac{D'}{\bar{D}} + \left(\frac{D'}{\bar{D}}\right)^2 - \dots \right]. \end{aligned} \quad (17)$$

Assuming $D' < \bar{D}$ so that terms of second order or higher inside the brackets on the right side of (17) can

be neglected, then

$$\frac{Q}{\rho C_p D} \approx \frac{(\bar{Q} + Q')}{\rho C_p \bar{D}} \left[1 - \frac{D'}{\bar{D}} \right], \quad (18)$$

and

$$\overline{\left(\frac{Q}{\rho C_p D}\right)} \approx \frac{\bar{Q}}{\rho C_p \bar{D}} - \frac{\overline{D'Q'}}{\rho C_p \bar{D}^2}. \quad (19)$$

Since

$$\left(\frac{Q}{\rho C_p D}\right)' = \frac{Q}{\rho C_p D} - \overline{\left(\frac{Q}{\rho C_p D}\right)}, \quad (20)$$

substituting (18) and (19) into (20) and rearranging terms gives

$$\left(\frac{Q}{\rho C_p D}\right)' \approx \frac{Q'}{\rho C_p \bar{D}} - \frac{1}{\rho C_p \bar{D}} \left[\frac{D'}{\bar{D}} (\bar{Q} + Q') - \frac{\overline{D'Q'}}{\bar{D}} \right]. \quad (21)$$

The left side of (21) denotes the anomalous temperature change due to nonadvective processes and is approximated by the sum of the three terms on the right side; the first term can be identified with the one

TABLE 1. Pattern correlation coefficients and rms differences between observed anomalous sea surface temperature changes and those computed from the effects of wind-driven ocean-surface currents (TADV'), heat transfer across the air-sea interface ($Q'/\rho C p D$), and the sum of TADV' and $Q'/\rho C p D$. The first group of figures for each month shows the results using the backward time-difference method to estimate the anomalous temperature changes, and the second group shows the results using the centered time-difference method.

		TADV'	$Q'/\rho C p D$	TADV' + $Q'/\rho C p D$
November 1969	$\Delta\theta'$ $i, i-1$	0.30 ¹ (09) ² 0.41 ³	0.21 (04)	0.30 (09) 0.53
	$\Delta\theta'$ $i+1, i-1$	0.19 (04) 0.38	0.70 (50) 0.17	0.44 (19) 0.48
	$\Delta\theta'$ $i, i-1$	0.77 (60) 0.32	0.54 (29) 0.36	0.81 (66) 0.30
December 1969	$\Delta\theta'$ $i+1, i-1$	0.48 (23) 0.37	0.71 (50) 0.18	0.66 (43) 0.38
	$\Delta\theta'$ $i, i-1$	0.12 (01) 0.46	0.03 (00) 0.36	0.12 (02) 0.52
	$\Delta\theta'$ $i+1, i-1$	0.11 (01) 0.36	0.20 (04) 0.20	0.20 (04) 0.43

¹ Pattern correlation coefficient.

² Reduction of variance.

³ Root-mean-square difference (°C).

used in this study to compute the anomalous temperature changes, the first term in the brackets represents the effect of fluctuations in mixed depth layer values,

TABLE 2. As in Table 1 except that the results are for seasons rather than months.

		TADV'	$Q'/\rho C p D$	TADV' + $Q'/\rho C p D$
Fall 1969	$\Delta\theta'$ $i, i-1$	0.30 (09) 0.58	-0.19 (04) 0.75	0.05 (00) 1.03
	$\Delta\theta'$ $i+1, i-1$	0.08 (01) 0.66	0.34 (12) 0.57	0.24 (06) 0.97
	$\Delta\theta'$ $i, i-1$	0.66 (43) 0.65	0.57 (33) 0.51	0.74 (55) 0.69
Winter 1969-70	$\Delta\theta'$ $i+1, i-1$	0.56 (32) 0.53	0.22 (05) 0.54	0.53 (28) 0.73
	$\Delta\theta'$ $i, i-1$	0.73 (54) 0.59	0.53 (28) 0.42	0.75 (56) 0.87
	$\Delta\theta'$ $i+1, i-1$	0.47 (22) 0.78	0.42 (18) 0.49	0.51 (26) 1.06
Spring 1970	$\Delta\theta'$ $i, i-1$	-0.08 (01) 0.81	0.54 (30) 0.67	0.44 (19) 0.80
	$\Delta\theta'$ $i+1, i-1$	0.28 (08) 0.46	0.54 (29) 0.66	0.61 (37) 0.73

TABLE 3. Pattern correlation coefficients and corresponding reduction of variances between heat transfer terms and observed variables.

		Total heat transfer Q'	Evaporative heat transfer Q_e'
Fall 1969	Q_e'	0.86 (74)	
	OBSW'	-0.56 (32)	-0.74 (55)
	cc'	0.21 (04)	
Winter 1969-70	Q_e'	0.97 (95)	
	OBSW'	-0.48 (23)	-0.48 (23)
	cc'	-0.07 (01)	
Spring 1970	Q_e'	0.89 (80)	
	OBSW'	-0.58 (34)	-0.56 (32)
	cc'	-0.52 (27)	
Summer 1970	Q_e'	0.59 (35)	
	OBSW'	-0.44 (20)	-0.12 (01)
	cc'	-0.56 (32)	
	Q_i'	0.50 (25)	

and the second term in the brackets represents the effect of possible correlations between anomalies in total heat transfer and mixed layer depth.

Order-of-magnitude specification errors resulting from the use of long-term mean values rather than monthly averaged observed values can be estimated by evaluating the relative magnitudes of the terms on the right side of (21) from data taken at Station PAPA between 1956 and 1963. The results of these computations are given in Table 4 (the terms were all multiplied by the common denominator $\rho C_p \bar{D}$ before the computations were made since only relative magnitudes are important). Values for each of the three terms were calculated for the four mid-season months, January, April, July and October, of five years for which all the necessary data were available.

In general, the values in Table 4 indicate that between-year mixed layer depth fluctuations have the greatest effect on the anomalous sea surface temperature changes during spring and summer, with the largest effects occurring when the new seasonal thermocline is developing. In fact, during April the term in (21) representing the effect of mixed layer depth anomalies on total heat transfer distribution is larger in four of the five years than the effect of total heat transfer anomalies. During July, it is larger for two of the five years, and on the average it is equally as important.

It appears that mixed layer depth anomalies have less effect on anomalous temperature changes during

TABLE 4. Relative magnitudes ($\text{cal cm}^{-2} \text{ day}^{-1}$) of the three terms on the right side of (21) using data from Station PAPA. The 1st column shows the total heat transfer anomalies Q' , the 2nd and 3rd columns show the effects of mixed layer depth anomalies on the total surface heat transfer distribution in the layer and percentage ratios of these effects to Q' , and the 4th and 5th columns show the effects of correlations between total heat transfer and mixed layer depth anomalies and the percentage ratios of these effects to Q' .

January					April						
Q'	$(D'/\bar{D}) \cdot (\bar{Q} + Q')$		$-\bar{D}'Q'/\bar{D}$		Q'	$(D'/\bar{D}) \cdot (\bar{Q} + Q')$		$-\bar{D}'Q'/\bar{D}$			
1956	-196	-48	24%	6.3	3%	1956	-8	-54	675%	-1.7	21%
1957	-45	13.3	30%	6.3	14%	1957	-5	4.4	88%	-1.7	3%
1961	41	0	0%	6.3	15%	1961	31	29.6	95%	-1.7	5%
1962	96	6	6%	6.3	6%	1962	-5	6.2	125%	-1.7	3%
1963	103	-1.7	2%	6.3	6%	1963	-14	20.6	147%	-1.7	12%
			12%		9%				226%		9%
July					October						
Q'	$(D'/\bar{D}) \cdot (\bar{Q} + Q')$		$-\bar{D}'Q'/\bar{D}$		Q'	$(D'/\bar{D}) \cdot (\bar{Q} + Q')$		$-\bar{D}'Q'/\bar{D}$			
1956	-44	-16.6	38%	10.1	22%	1956	-70	39.4	56%	-8.1	11%
1957	-80	44.4	56%	10.1	12%	1957	15	3.2	21%	-8.1	53%
1961	27	-71.2	264%	10.1	37%	1961	41	0	0%	-8.1	19%
1962	60	19.7	33%	10.1	16%	1962	82	-26.3	31%	-8.1	9%
1963	28	-34.2	122%	10.1	35%	1963	-68	-24.4	36%	-8.1	11%
			102%		24%				29%		21%

fall and winter, as indicated by the values shown for October and January. However, they cannot be overlooked since in some years these effects were 30–56% as large as those of total surface heat transfer anomalies. During October the average of the ratios is 29%, or the average effects of mixed layer depth anomalies are nearly one-third as large as the average effects of total heat transfer anomalies.

The values in Table 4 involving correlations between mixed layer depth and total heat transfer anomalies are smaller than those for either of the two considered separately. However, the correlation effects cannot necessarily be neglected in July and October since they average about one-fifth as large as the total surface heat transfer anomalies in these months, and are nearly as large as the effects of mixed layer depth anomalies in October.

7. Summary

In Section 2, a specification method was developed that relates the change in sea surface temperature anomalies between times t_1 and t_2 to anomalies of temperature advection and non-advective heat transfer across the air-sea interface integrated over the interval t_1 to t_2 .

In order to test the adequacy of the method, monthly and seasonally averaged marine weather observations from 1961–70 were used to compute monthly and seasonal anomalies of sea surface temperature change, temperature advection, and non-advective heat transfer over a network of grid points covering the eastern North Pacific. Descriptive and statistical comparisons were then made between observed changes in sea surface temperature anomaly patterns and those computed using the specification procedure. The results indicate

quite clearly that both advective and non-advective processes are important in determining the nature of temperature anomalies in the surface layer of the ocean. Their relative importance appears to depend upon the initial thermal state of the layer and the subsequent character of the overlying atmospheric circulation.

The highest correlations between observed and specified anomalous changes were obtained for periods when anomalous atmospheric activity over the eastern North Pacific was intense and quite persistent. Under these conditions, computed temperature changes are probably more representative of those that actually occur since errors resulting from the use of monthly or seasonally averaged data in the nonlinear transfer equations become less serious.

Comparisons between the observed and specified seasonal anomaly patterns indicate that temperature advection has a greater effect in determining anomalous sea surface temperature changes in winter and spring, while non-advective processes appear to have a greater effect in summer and fall.

In Section 6, a perturbation-type analysis of the non-advective heating expression $Q'/(\rho C_p D)$ was made in order to estimate the effects of using long-term mean values of the mixed layer depth D instead of observed values in computing anomalous sea surface temperature patterns. In order to eliminate these errors and improve specification results, data on the vertical temperature structure of the ocean will have to be obtained so that mixed layer depths can be determined for time periods that correspond to those used in a particular specification method.

Finally, an important factor to keep in mind is that air-sea interaction processes do not conform to any standard time scales such as months, seasons, etc. In order to improve our knowledge of these processes, time

scales that represent the varying atmospheric circulation periods will have to be examined. The descriptions and statistics presented here only point out that known processes are having effects on large time and space scales, and no attempt has been made to explain all the features of these complete interactions.

Acknowledgments. I thank Mr. James A. Renner for his invaluable assistance in data preparation, computer programming, and initial drafting of the figures, Mr. Kenneth S. Raymond for the final drafting of the figures, and Miss Joanne Webber for typing the manuscript.

APPENDIX

Finite Difference Approximations

In order to test the validity of the relationship expressed by (15) and the assumptions made in determining the heat flux components, $\partial\theta/\partial t$ needs to be approximated by some finite difference scheme, $\partial\theta/\partial t \approx \Delta\theta/\Delta t$, where $\Delta\theta$ denotes the change in sea surface temperature over a time interval Δt . Since monthly averaged data were used to compute the terms on the right side of (15), $\Delta\theta/\Delta t$ should be determined from the temperature values at the beginning and end of each month. However, this information was not available, and it was necessary to approximate $\Delta\theta/\Delta t$ using the monthly averaged temperature values.

The first approximation method used is a "backward" finite-difference scheme in which $\Delta\theta/\Delta t$ is computed from the difference between the value of θ for the month over which the approximation is desired and the value of θ for the previous month. This scheme is represented by $\frac{\Delta\theta}{i, i-1}$ where i denotes the present month and $i-1$ denotes the previous month. Monthly averaged values, 10-year mean values, and monthly anomaly values were computed using the 120 months in the 10-year data record.

The other method used in approximating $\Delta\theta/\Delta t$ is a "centered" finite-difference scheme in which half the difference between the value of θ for the month subsequent to the one over which the approximation is desired and the value of θ for the previous month is computed. This scheme is represented by $\frac{\Delta\theta}{i+1, i-1}$ where $i+1$ denotes the subsequent month, and $i-1$ denotes the previous month. Again, monthly averaged

values, 10-year mean values, and monthly anomaly values were computed.

A major drawback in using either of these approximations is that the values obtained might be strongly biased by unusually anomalous events occurring in one of the months previous or subsequent to the one for which $\Delta\theta/\Delta t$ is needed.

REFERENCES

- Arthur, R. S., 1966: Estimation of mean monthly anomalies of sea-surface temperature. *J. Geophys. Res.*, **71**, 2689-2690.
- Clark, N. E., 1967: Report on an investigation of large-scale heat transfer processes and fluctuations of sea-surface temperature in the North Pacific Ocean. Ph.D. thesis, M. I. T., 148 pp.
- , 1968: Specification of sea-surface temperature anomalies. Project. Rept., National Marine Fisheries Services, La Jolla, Calif.
- Eber, L. E., 1961: Effects of wind-induced advection on sea-surface temperature. *J. Geophys. Res.*, **66**, 839-844.
- Green, R. A., 1970: The weather and circulation of November 1969. *Mon. Wea. Rev.*, **98**, 170-174.
- Jacob, W. C., 1967: Numerical semiprediction of monthly mean sea surface temperature. *J. Geophys. Res.*, **72**, 1681-1689.
- Johnson, J. H., G. A. Flittner and M. W. Cline, 1965: Automatic data processing. Program for marine, synoptic radio weather reports. Spec. Sci. Rept. Fisheries No. 503, Fish and Wildlife Service.
- Kraus, E. B., and R. E. Morrison, 1966: Local interactions between the sea and air at monthly and annual time scales. *Quart. J. Roy. Meteor. Soc.*, **92**, 114-127.
- Namias, J., 1959: Recent seasonal interactions between North Pacific waters and the overlying atmospheric circulation. *J. Geophys. Res.*, **64**, 631-646.
- , 1963: Large-scale air-sea interactions over the North Pacific from summer 1962 through the subsequent winter. *J. Geophys. Res.*, **68**, 6171-6186.
- , 1965: Macroscopic association between mean monthly sea-surface temperature and the overlying winds. *J. Geophys. Res.*, **70**, 2307-2318.
- , 1969: Seasonal interactions between the North Pacific Ocean and the atmosphere during the 1960's. *Mon. Wea. Rev.*, **97**, 173-192.
- , 1970: Macroscale variations in sea-surface temperatures in the North Pacific. *J. Geophys. Res.*, **75**, 565-582.
- , 1971: The 1968-69 winter as an outgrowth of sea and air coupling during antecedent seasons. *J. Phys. Oceanogr.*, **1**, 65-81.
- Pattullo, J. G., and J. D. Cochrane, 1951: Monthly thermal condition charts for the North Pacific Ocean. MS Rept. No. 3, Bathythermograph Section, Scripps Inst. Oceanogr., 30 pp.
- Posey, J. W., 1970: The weather and circulation of December 1969. *Mon. Wea. Rev.*, **98**, 253-258.
- Wagner, A. J., 1970: The weather and circulation of January 1970. *Mon. Wea. Rev.*, **98**, 328-334.